

Remarkable muscles, remarkable locomotion in desert dwelling wildebeest

Nancy A. Curtin¹, Hattie L.A. Bartlam-Brooks¹, Tatjana Y. Hubel¹, John C. Lowe¹, Anthony R. Gardner-Medwin², Emily Bennitt³, Stephen J. Amos¹, Maja Lorenc¹, Timothy G. West¹ and Alan M. Wilson¹

¹Structure & Motion Lab, Royal Veterinary College, University of London, Hatfield, UK. ²Dept Neuroscience, Physiology & Pharmacology, University College London, London, UK ³Okavango Research Institute, University of Botswana, Maun, Botswana.

doi: 10.1038/s41586-018-0602-4

<https://www.nature.com/articles/s41586-018-0602-4>

Large mammals that live in arid/desert environments can cope with seasonal and local variations in rainfall, food and climate¹ by moving long distances, often without reliable water or food en route. An animal's capacity for this long distance travel is substantially dependent on the rate of energy utilisation and hence heat production during locomotion - the cost of transport, COT²⁻⁴. Terrestrial COT is much higher than for flying (7.5 times) and swimming (20 times)⁴. Terrestrial migrants are usually large^{1,2,3} with anatomical specialisations for economical locomotion⁵⁻⁹ because COT reduces with increasing size and limb length^{5,6,7}. Here we used GPS tracking collars¹⁰ with movement and environmental sensors to show that blue wildebeest (*Connochaetes taurinus*, 220 kg) living in a hot arid environment in Northern Botswana walked up to 80 km over five days without drinking. They predominantly travelled during the day and locomotion appeared unaffected by temperature and humidity although some behavioural thermoregulation was apparent. We measured power and efficiency of work production (mechanical work and heat production) during cyclic contractions of intact muscle biopsies from *flexor carpi ulnaris* of wildebeest and domestic cows (*Bos taurus*, 760 kg), a comparable sedentary ruminant. The energetic costs of isometric contraction (activation and force generation) in wildebeest and cows were similar to published values for smaller mammals. Wildebeest muscle was substantially more efficient (62.6%) than the same muscle from substantially larger cows (41.8%) and comparable measurements made in smaller mammals (mouse 34%¹¹, rabbit 27%). These are the first direct energetic measurements on intact muscle fibres from large mammals and we use them to model the contribution of high working efficiency of wildebeest muscle to minimising thermoregulatory challenge during their long migrations under hot arid conditions.

We set out to test the hypothesis that wildebeest undertake long-range locomotion from grazing sites to water sources and that their muscle is optimised to deliver a low COT. We chose blue wildebeest living in the Makgadikgadi Pans National Park in Botswana because water is sparse and in known locations and grazing limited.

Wildebeest were captured by darting from a helicopter and fitted with tracking collars of our own design¹⁰ containing GPS, 3D accelerometer, 3D gyroscope, 3D magnetometer, a humidity sensor and a black globe thermometer¹² (to measure combined effect of solar radiation, air temperature and air velocity for the animal) (Fig. 1a, Methods). Collar mass was 1050 g, 0.5% of body mass. After 18 months collars released automatically, dropoff failures were recovered by re-darting, and 17 of the 20 deployed collars were recovered (to date)

(Extended Data Table 1). During tranquilisation, a muscle biopsy with aponeurosis at each end was removed from the *flexor carpi ulnaris* (a forelimb flexor) muscle of six wildebeest (leg length to *serratus ventralis* insertion 1.09 m, approximate body mass 220 kg) under open aseptic conditions and immediately returned to the field lab by helicopter. Equivalent biopsies were collected from *flexor carpi ulnaris* of seven adult cows (leg length to *serratus* insertion 1.28 m, 770 kg) at a UK abattoir. Work was approved by RVC Ethics & Welfare Committee (RVC 2013 1233).

In the dry season range wildebeest drank (exclusively) from the Boteti river, usually every 2 - 3 days however thirteen out of sixteen individuals went 4 days between drinking events at least once, and seven individuals went 5 days. (Fig. 1b,c,g,i,j,n). The wildebeest grazed 5-15 km away from the river and covered 20-40 km between drinks (Fig. 1d,f,j) and they consistently drank in the middle of the day (time clusters around multiples of 24 hours, Fig. 1g,j,m). Each year wildebeest migrated to and from the wet season range, 60-80 km over 3 or 4 days across a waterless environment. This daily distance (Fig. 1e,f,h,i) was further than most non-migrating wildebeest travel.

Humidity peaked in the wet season and dropped below 12% in the dry season (median for September, Fig. 1o). Globe temperature on the collar peaked in October (Fig. 1p). Neither humidity or globe temperature appeared to curtail maximum distance travelled (Fig. 1k,l). Data from two fixed weather stations on the walking route (Fig. 1b) recorded considerably ($5.6 \pm \text{SD } 0.6$ °C) higher peak and lower ($3.6 \pm \text{SD } 1.1$ °C) minimum globe temperatures than the animal collars (Extended Data Fig. 1) indicating behavioural thermoregulation at both temperature extremes. The mean daily maximum, by month, exceeded 38°C in nine out of twelve months.

These data show that wildebeest are able to cover up to 80 km and last up to five days without drinking, contrary to published observations which report a requirement for daily drinking¹³. This pattern of activity is necessary in the studied environment due to depletion of grazing areas close to the only permanent water source as well as the bi-annual migration across a waterless environment between seasonal ranges. This behaviour persisted even in late dry season when daytime temperature was high and low humidity would maximise respiratory water loss.

Almost all locomotion (97% of total distance) was at a slow walk within a narrow speed range centred around a preferred speed of 1.14 m s^{-1} and stride frequency centred around 1.00 Hz (Fig. 1q,r). This corresponds to a dimensionless speed of 0.35, (leg length 1.09 m), which is around optimum for mechanical COT minimisation^{14,15}. Occasional short bursts of faster locomotion at up to 15 m s^{-1} occurred with approximately double the stride frequency (peak of 1.92 Hz at 4 ms^{-1}) accounting for 3% of daily distance travelled. The intermediate gait of trotting was very rarely used: only 5% of the faster non-walking strides (0.15% of total).

We cycled muscle biopsies at 0.5 Hz at 25°C, which approximated to temperature-corrected wildebeest walking stride frequency (Fig. 1r) and recorded force, length and heat production. We systematically varied the stimulation duration (duty cycle, DC) and stimulation phase (start of stimulation relative to start of shortening, Extended Data Fig. 2). Figure 2 shows the stimulus pattern that elicited high power and efficiency from a wildebeest fibre bundle.

Successful experiments were performed on five fibre bundles from four wildebeest and five bundles from five cows.

Power (Fig. 3a,e) increased with stimulation duration (between DC 0.1 and 0.3) and the power curve shifted to the left and became narrower. Peak power was produced when stimulation and shortening started at the same time (phase zero). Extended Data Table 2; N values Extended Data Fig. 3; individual data points.

Impulse (integral of time and active stress) varied with DC and with phase (Fig. 3c,g) and the largest impulse was produced under isometric conditions. When more of the stimulation occurred during stretch (phase became more negative) the impulse was higher (Fig. 3c,g) and the cost per unit of impulse lower (Fig. 3d,h). For wildebeest the minimum cost per unit of impulse during cyclic movement ($0.056 \text{ (J kg}^{-1}\text{)/(kPa s)} \pm \text{sem } 0.011, n=4$) was slightly less than for isometric contraction ($0.068 \text{ (J kg}^{-1}\text{)/(kPa s)} \pm \text{sem } 0.021, n=4$), though the stimulation duration was different (Extended Data Table 3a). The cost of impulse under isometric conditions for wildebeest muscle was similar to that derived from published data for rats, and that for cow (Extended Data Table 3b).

Three wildebeest fibre bundles performed a fatiguing series of contractions (see Methods) which reduced force considerably (Fig. 3i), but force producing capacity was completely restored after a recovery period without stimulation (Fig. 3j). This muscle resilience is high compared with equivalent data for other species and it may reflect low metabolic demands of the fibres and/or good intra-muscle buffering of pH. The muscles were observed to be very red in appearance, suggesting substantial oxidative capacity as observed histochemically in somewhat similar black wildebeest (*Connochaetes gnou*)¹⁶.

For both wildebeest and cow the efficiency of net work production was strongly dependent on stimulation phase and peaked at either -0.1 or 0.0 for all duty cycles (Fig. 3b,f). Efficiency values (Extended Data Fig. 4, Extended Data Table 4) are enthalpy efficiencies; (mechanical power)/(sum of heat production rate and mechanical power). Furthermore they are *initial* enthalpy efficiency values, meaning that the enthalpy is produced during the contractions and is from ATP and phosphocreatine use, coupled by the creatine kinase reaction. The mean maximum efficiencies we measured for wildebeest muscle, $62.6\% \pm \text{sem } 2.3$ ($n=4$), and for cow muscle, $41.8\% \pm \text{sem } 1.2$ ($n=5$) are high. The wildebeest value is higher than any locomotor muscle except that from tortoise¹⁷ (See Extended Data Table 5), an animal fabled for slow locomotor speed and good endurance. Tortoise have long stance times and low stride frequency¹⁸. The cow is by far the largest mammal and the wildebeest the only long-distance locomotion specialist which have been the subject for such energetic measurements. Based on their larger body mass the cows would be expected to have a COT 44% lower than wildebeest⁵.

The mechanisms responsible for the high initial enthalpy efficiency could arise from 1) the ATP-driven Ca^{2+} uptake into the SR, and 2) the cross-bridge cycle in which one ATP is used in each round of attachment, work-producing filament sliding, and detachment. We used the principles set out by Barclay¹⁹ (see Methods) to compare the work the cross-bridge actually did with the amount of work it could theoretically do; this is the efficiency of the fundamental contractile event. Mechanistically, does the cross-bridge attach and detach at

appropriate locations to yield maximum work? In tortoise muscle, each cross-bridge cycle produces 45.8 zJ of work ($z=10^{-21}$), amounting to 92% of the theoretically possible 50 zJ, with the remaining 8% degraded to heat¹⁷ (see Extended Data Table 6) and the wildebeest cross-bridge generates work amounting to between 74 and 86% of the theoretically possible 50 zJ, with the rest appearing as heat. For cow the corresponding calculation gives cross-bridge work between 50 and 57% of the theoretical maximum. The high efficiency of cross-bridge cycle in wildebeest muscle mean that work is produced with relatively low heat production. Thus the efficiency of the cross-bridge cycle itself has an important role supporting the wildebeest's ability to function effectively in its environment. The use of a slow walking gait with high DC and low stride frequency likely exploits this efficiency to the full.

Energy required (above resting metabolism) for a 220 kg wildebeest walking 20km/day (Fig. 1j) would be around 0.379 MJ/km or 7.58 MJ/day, requiring an additional oxygen consumption of 18.9 L/km⁵ (Methods). Assuming a 5% oxygen extraction from air²⁰ this requires an additional ventilation of 378 L/km and a consequent additional water loss in expired air of 15.2 mL/km or 304 mL/day. This is largely offset by 11.5 mL/km (230 mL/day) water generated through metabolism, leading to a net water loss of just 3.7 mL/km or 74 mL/day.

Heat accumulation can be a major issue for a desert-dwelling animal^{1,21}. Without heat dissipation the heat energy from 20 km walking (7.58 MJ) would raise body temperature by an intolerable 10°C. When ambient temperature exceeds body temperature (Fig. 1p, Extended Data Fig. 1) thermoregulation can only be achieved by evaporative cooling and in level locomotion almost all energy used by muscles converts, directly or indirectly, to heat within the animal's body.

The behavioural thermoregulation reported above suggests wildebeest avoided direct heat, eg by standing in the shade or in moving air but this may not be concomitant with long distance movement. An additional way to minimise temperature problems would be to move at dawn, dusk or overnight, yet nearly all long-distance movements occurred during warm daylight hours, arriving at the river late morning and leaving mid-afternoon (Fig. 1m). This behaviour possibly reduces the risk of predation by lions²².

In order to dissipate all the extra heat (7.58 MJ) generated by walking 20 km by evaporation, the 220 kg wildebeest would need to evaporate 3.36 L/day. This is substantially more than the 0.23 L/day generated chemically from the extra metabolism. The net loss (3.13 L/day, or 1.4% body mass/day) would be a significant dehydration load. If the same work in transport were performed by muscle with cow muscle enthalpy efficiency (41.8% vs 62.6%) the energetic cost of work, respiratory and thermoregulatory water loss would all be 50% greater (4.7 L/day, 2.1% body mass/day). Additional water depletion will occur associated with basal metabolism, possibly as much as 5.4% of body mass/day - the observed water intake of grazing wildebeest²³. Animals become debilitated through dehydration when they reach around 20% body mass loss²⁴ corresponding to between three and four days between drinks.

We suggest that wildebeest, particularly in migration, may gain significant range under hot arid conditions as a result of having highly efficient muscles.

In summary, wildebeest, whilst not considered extreme arid environment specialists, can undertake long journeys in the absence of water in hot dry conditions and frequently spend three and occasionally up to five days without drinking. This requires them to have a low COT which is likely delivered, in part, by muscles that are specialised at the level of the cross-bridge to deliver more mechanical work and release less heat from each ATP molecule split than any mammalian muscle studied to date. Equivalent data for cow muscle shows that the muscle specialisation is not simply attributable to animal size. The economical muscles are therefore likely to be critical in minimising heat accumulation and enabling the nomadic lifestyle of these wildebeest and exploitation of distant pastures particularly during periods of nutritional deprivation and/or high ambient temperature. Such physiological adaptations may be critical to surviving in a changing world.

References

- 1 Schmidt-Nielsen, K. *Desert animals: Physiological problems of heat and water*. Oxford: Clarendon Press; 1965.
- 2 Hedenström, A. Optimal migration strategies in animals that run: a range equation and its consequences. *Anim Behav.* **66**, 631-636 (2003).
- 3 Hein, A.M., Hou, C., Gillooly, J.F. Energetic and biomechanical constraints on animal migration distance. *Ecol Lett.* **15**, 104-110 (2012).
- 4 Tucker, V.A. The Energetic Cost of Moving About: Walking and running are extremely inefficient forms of locomotion. Much greater efficiency is achieved by birds, fish—and bicyclists. *Am Sci.* **63**, 413-419 (1975).
- 5 Taylor, C.R., Heglund, N.C., Maloiy, G.M.O. Energetics and mechanics of terrestrial locomotion. I. Metabolic energy consumption as a function of speed and body size in birds and mammals. *J Exp Biol.* **97**, 1-21 (1982).
- 6 Kram, R., Taylor, C.R. Energetics of running: a new perspective. *Nature* **346**, 265-267 (1990).
- 7 Wilson, A.M., Watson, J.C., Lichtwark, G.A. Biomechanics: A catapult action for rapid limb protraction. *Nature* **421**, 35-36 (2003).
- 8 Alexander, R., Maloiy, G.M.O., Njau, R., Jayes, A. Mechanics of running of the ostrich (*Struthio camelus*). *J Zool.* **187**, 169-178 (1979).
- 9 Alexander, R., Maloiy, G.M.O., Ker, R., Jayes, A., Warui, C. The role of tendon elasticity in the locomotion of the camel (*Camelus dromedarius*). *J Zool.* **198**, 293-313 (1982).
- 10 Wilson, A.M., Lowe, J.C., Roskilly, K., Hudson, P.E., Golabek, K.A., McNutt, J.W. Locomotion dynamics of hunting in wild cheetahs. *Nature* **498**, 185-189 (2013).
- 11 Barclay, C.J. Efficiency of fast-and slow-twitch muscles of the mouse performing cyclic contractions. *J Exp Biol.* **193**, 65-78 (1994).

- 12 Hetem, R.S., Maloney, S.K., Fuller, A., Meyer, L.C., Mitchell, D. Validation of a biotelemetric technique, using ambulatory miniature black globe thermometers, to quantify thermoregulatory behaviour in ungulates. *J Exp Zool A Ecol Genet Physiol.* **307**, 342-356 (2007).
- 13 Estes, R. *The behavior guide to African mammals*. Vol. 64 University of California Press Berkeley; 1991.
- 14 Kuo, A.D. A simple model of bipedal walking predicts the preferred speed–step length relationship. *J Biomech Eng.* **123**, 264-269 (2001).
- 15 Bertram, J.E. Constrained optimization in human walking: cost minimization and gait plasticity. *J Exp Biol.* **208**, 979-991 (2005).
- 16 Kohn, T.A., Curry, J.W., Noakes, T.D. Black wildebeest skeletal muscle exhibits high oxidative capacity and a high proportion of type IIX fibres. *J Exp Biol.* **214**, 4041-4047 (2011).
- 17 Woledge, R. The energetics of tortoise muscle. *J Physiol.* **197**, 685-707 (1968).
- 18 Williams, T.L. Experimental analysis of the gait and frequency of locomotion in the tortoise, with a simple mathematical description. *J Physiol.* **310**, 307-20 (1981).
- 19 Barclay, C.J. Energetics of contraction. *Compr Physiol.* **5**, 961-995 (2015).
- 20 Butler, P., Woakes, A., Smale, K., Roberts, C., Hillidge, C., Snow, D. et al. Respiratory and cardiovascular adjustments during exercise of increasing intensity and during recovery in thoroughbred racehorses. *J Exp Biol.* **179**, 159-180 (1993).
- 21 Hetem, R.S., Maloney, S.K., Fuller, A., Mitchell, D. Heterothermy in large mammals: inevitable or implemented? *Biol Rev.* **91**, 187-205 (2016).
- 22 Valeix, M., Loveridge, A., Chamaillé-Jammes, S., Davidson, Z., Murindagomo, F., Fritz, H. et al. Behavioral adjustments of African herbivores to predation risk by lions: spatiotemporal variations influence habitat use. *Ecology* **90**, 23-30 (2009).
- 23 Macfarlane, W., Howard, B., Haines, H., Kennedy, P., Sharpe, C. Hierarchy of water and energy turnover of desert mammals. *Nature* **234**, 483-484 (1971).
- 24 Maloiy, G.M.O. Water economy of the Somali donkey. *Am J Physiol* **219**, 1522-1527 (1970).

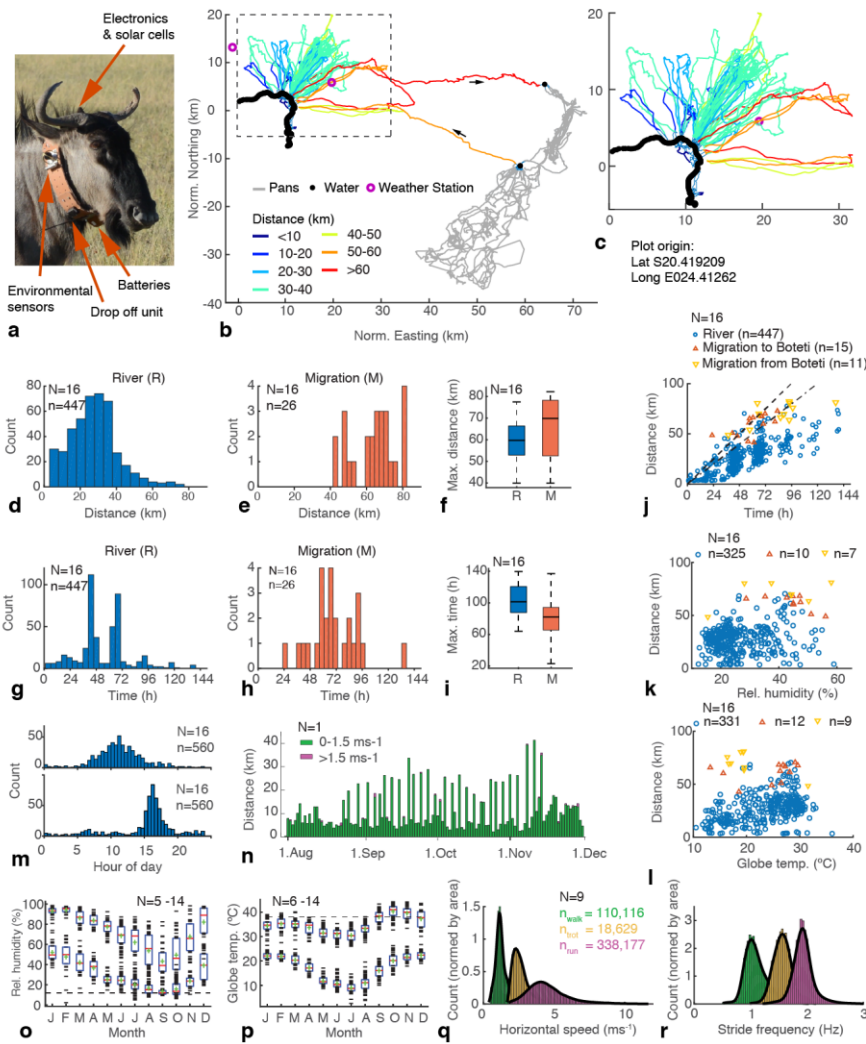


Figure 1. Locomotion of desert wildebeest. (a) collared wildebeest. (b) typical wildebeest range, black is Boteti river, grazing ground forays coloured by distance between drinking events. Migratory journeys between dry and wet season range (grey) are colour coded by distance between drinks. (c) Dry season range. (d) Distance covered between drinks at river and (e) during migrations. N = number of animals, n = number of journeys) (f) Distribution (median, IQR and range) of longest interdrink distances for each individual. (g,h) Time between drinks showing circadian drinking pattern. (i) as (f) for longest individual interdrink times. (j) Distance covered vs time taken for each journey, dashed lines represent 20 and 25 km/day. (k) Distance between drinks against mean humidity during the period, blue: dry range, red: migration to river, yellow: migration from river. (l) as (k) for mean temperature. (m) time of arrival at, and departure from the river. (n) Daily distance for one wildebeest during dry season showing pattern of a long walk to/from the river interspersed with one or two grazing days. Green=walking purple=faster locomotion. (o) daily maximum and minimum ambient humidity from median of all animal mounted sensors, grouped by month. Red line: median, + is mean, box is IQR. (p) daily maximum and minimum globe temperature derived as in o. (q). Speeds (q) and stride frequencies (r) used derived from high rate data only (nine collars, number of strides given) and subdivided into gaits (green-walk, yellow-trot, purple-canter/gallop) with normalisation for equal area under curve for each gait.

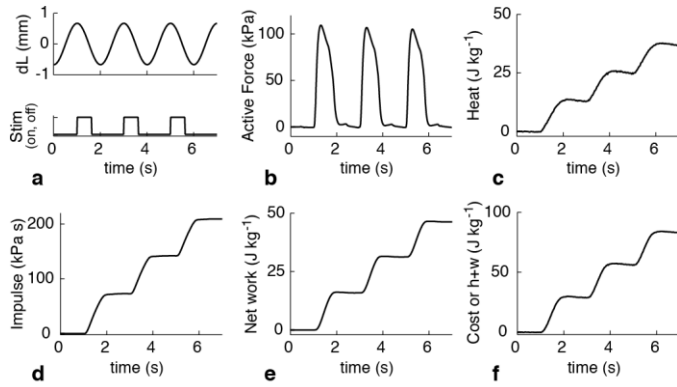


Figure 2. Example records. (wildebeest - bundle 4A, DC 0.3, phase 0). **a**, Length change and stimulus pattern imposed. **b**, active stress and **c**, heat produced by the fibre bundle. **d**, **e** and **f** show quantities calculated from **a**, **b** and **c**. **d**, impulse = integral of active stress and time. **e**, net work = integral of active force and length change. **f**, cost evaluated as the total energy = heat production+net work. For three cycles, the heat was 36.22 (panel c), net work was 46.27 (panel e), and heat+net work was 82.50 (panel f). Therefore efficiency = net work/(heat+net work) = 56.1% (46.27/82.50). This efficiency point is shown in Extended Data Fig. 4d, square at phase 0. Active force is expressed relative to the cross-sectional area of the bundle, and heat, work and cost are expressed relative to the mass of the bundle. Muscle fibre length 7.1 mm, fibre bundle mass 9.02 mg. Net work over three cycles was 46.3 J kg⁻¹, an average cycle power of 7.7 W kg⁻¹.

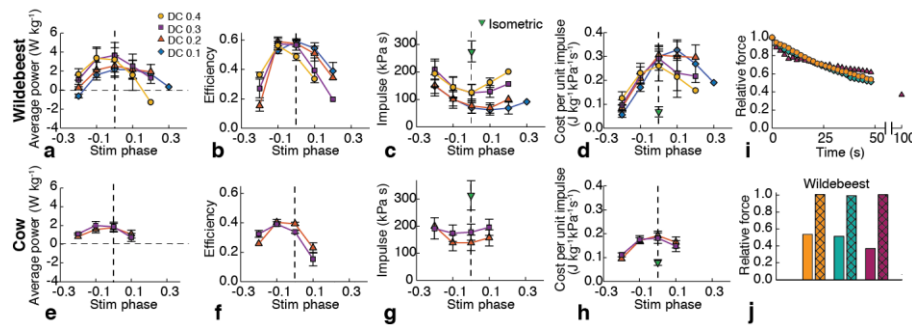


Figure 3. Muscle mechanical and energetic performance. **a-d** wildebeest; **e-h** cow. Relationship between stimulus phase and mechanical and energetic outputs during three cycles of movement at 0.5 Hz and different stimulus duty cycles: (DC). Isometric contractions at DC 0.4 down triangle. **a** and **e**, Average power. **b** and **f**, Efficiency = power per rate of heat+work output. **c** and **g**, Impulse = integral of active stress and time. **d** and **h**, Cost per unit of impulse = (heat+work) impulse⁻¹. Mean ± sem, n=3 to 5 Mean only, when n=2. n given in Extended Data Table 2. **i**, Fatigue of wildebeest fibre bundles. Peak force in 25 or 50 isometric contractions (at 2 s intervals, DC 0.4). Peak force is normalised to the 1st contraction. **j**, Extent of fatigue and recovery. Peak force in last contraction (plain bars) and after the recovery period of 10 and 30 min respectively (hatched).

Acknowledgments: Roger Woledge for contributing to early design of experiments. Chris Barclay for helping us fabricate the thermocouple elements. Field assistants Naomi Terry and Megan Claase. Anna Wilson for logistical support and editorial contributions. Michael Flyman, Department of Wildlife and National Parks for his support and enthusiasm and James O’Conner and Pat O’Riordan, Dawn Meats, Bedford for enabling cow muscle collection. Funding from EPSRC (EP/H013016/1), BBSRC (BB/J018007/1) and ERC (323041). Botswana Research Permit EWT 8/36/4 held by AW and AW was a registered Botswana veterinarian.

Author Contributions: AW, NC and HB conceived, designed and led the study, HBB, EB led and organised field work. AW performed veterinary procedures and biopsies. NC, AGM, ML, and TW undertook muscle experiments and NC and AGM analysed and interpreted muscle data. JL,AW,SA designed and built collars and weather stations. TH, AW and HBB analysed and interpreted collar data, AW made water balance model and AW and NC wrote paper with input from all authors. The authors declare no competing financial interests.

Author Information: Reprints and permissions information is available. Correspondence and requests should be addressed to ncurtin@rvc.ac.uk or awilson@rvc.ac.uk.

Methods

Animals

Custom-made GPS collars were deployed on twenty female wildebeest that were collared in their wet season range in the Makgadikgadi Pan National Park in Botswana in May 2016. Animals were free-darted from a Robinson R44 helicopter by AW, a Botswana registered Veterinary Surgeon, using 5 mg etorphine hydrochloride (M99, Novartis, Kempton Park, South Africa), 80 mg azaperone (Kyron Laboratories, Benrose, South Africa), 1700 IU lyophilized hyalase (Kyron Laboratories). For reversal diprenorphine (Novartis) and/or naltrexone (Kyron Laboratories) were used. Timed-release drop-offs (TRD, Lotek, Newmarket, Canada) released collars automatically after 18 months. Two collars remain deployed at time of writing, 16 collars were retrieved and two lost. Data were recorded for 17 animals for durations varying due to difficulties downloading large data sets, collar failure and animal death (Extended Data Table 1). Fifty-nine percent of drop-offs failed and those collars were recovered by re-darting via helicopter.

Open biopsies were obtained under aseptic conditions from the *flexor carpi ulnaris* muscle. Animals were treated with a long acting antibiotic (Norocillin LA, Norbrook, 6 mg/kg benzathine penicillin, 4.5 mg/kg procaine penicillin IM) and a nonsteroidal anti-inflammatory drug (Metacam, Boehringer Ingelheim Ltd, 0.5 mg meloxicam/kg body weight IM). The *flexor carpi ulnaris* muscle was chosen because it was superficial, accessible, unipennate and a few millimetres thick. The fibres run between aponeurosis sheets and the fibre length was appropriate for mounting in the thermopile.

Collars

Collars used in this study were designed, engineered and assembled at the RVC^{10,25} (Fig. 1a). Collars were fitted with a VHF tracking transmitter (African Wildlife Tracking, Pretoria, South Africa), one Lithium Polymer rechargeable battery (Active Robots, Radstock, UK), charged by a solar cell array consisting of ten monocrystalline silicon solar cells (KXOB22-12X1, Ixys, Milpitas, USA) and two standby D cell Lithium Thionyl Chloride batteries (LSH20T, Saft Groupe SA, Bagnolet, France). They were further equipped with a GPS module (M8N GPS module; u-Blox AG, Thalwil, Switzerland), a 6-axis Inertial Measurement Unit incorporating a 3-axis accelerometer and a 3-axis gyroscope (MPU-6050, TDK-Invensense, San Jose, CA, USA), a separate low power 3-axis accelerometer (MMA8652, NXP Semiconductors, Eindhoven, Netherlands), a 3-axis Magnetometer (HMC5883, Honeywell International Inc, Plymouth, MN, USA) and an ambient light sensor (TSL2591, Ams AG, Unterpremstaetten, Austria). Additionally, the collars were outfitted with an environmental measurement unit which recorded humidity, ambient temperature and globe temperature every 30 seconds. The unit was comprised of a humidity sensor (HIH6131, Honeywell Inc, Golden Valley, MN, USA), and two temperature sensors (MCP9808, Microchip Technology Inc, Chandler, AZ, USA), one positioned near the humidity sensor inside a silvered, cross drilled metal tube for ambient temperature measurement and the other mounted in the centre of a miniature blackened 30 mm globe (Press Spinning & Stamping Co., Cape Town, South Africa) for derivation of mean radiant temperature¹². The unit was connected on an I2C bus via a gateway and protected power switch which prevented any damage interfering with main collar operation.

GPS positions were recorded at five minute intervals. During June, October and January (cold dry, hot dry, hot wet season) collars switched dynamically to a sample rate of 5 Hz (50 Hz IMU) during higher speed locomotion when triggered by the animal's activity^{10,25}. The GPS module provides an estimate for each position and an instantaneous velocity data point (position accuracy: 0.95 m (median SD), horizontal speed accuracy: 0.30 m s⁻¹ (median SD)). During higher speed locomotion IMU and GPS are Kalman fused to give substantially higher accuracy data¹⁰ (below).

Fixed-position weather stations consisted of electronic boards and batteries (same as in collars) mounted in clear polycarbonate cases with a temperature and a humidity sensor contained within a Stevenson Screen 3D printed of polylactic acid (PLA). These were mounted approximately 1.25 metres off the ground (to match collar height) on dead trees at locations shown on Figure 1b. Data were recorded every 30 seconds.

Movement and Location

Collar analysis was conducted in MATLAB (Mathworks Inc., Natick, MA, USA). GPS position data with a horizontal accuracy estimate greater than 15 m were excluded from the analysis. Location was divided into an area close to the Boteti river where most animals spend the dry season, with the river being the only water source, and the pans to the East where they spend the wet season. Animals migrate from the river to the pans at the beginning of the wet season (November) and back to the Boteti river at the beginning of the dry season when the pans dry out (April-May). Direct distance between river and closest edge of the

pans is about 40-55 km. During the wet season water is readily available in the pans, therefore we concentrated our analyses on times at the river and during migration between river and pans to calculate distance and time between drinking. Times the animals spent in the pans were excluded from the analysis. One animal spent a whole year at the pans bringing the number of animals used for all analysis, except gait data, to 16.

The location of the river was derived from Google Earth by generating a path along the river and saving the coordinates as a CSV file.

Drinking was assumed to have occurred whenever the wildebeest was less than 500 m from the river. Distance and time between drinking was calculated based on the cumulative distance/time between two drinking events. Paths between drinking events were colour-coded based on distance covered (Fig 1 b,c) by summing displacement between five minute GPS fixes which will be an underestimate²⁶.

Migration events were identified manually and only analysed if the first/last drinking event in the pans could reliably be identified as a known water hole. Out of 47 migrations, these criteria were met and distance and time calculated for 15 migrations to the pans and 11 from the pans (Fig 1e,h).

Maximum distance and maximum time between drinking were calculated for each individual during times at the river and migration; median values over all individuals were displayed in Fig. 1f,i.

Humidity and ambient temperature were interpolated to give a value coincident with the five minute GPS position and then averaged over the time between drinking events.

Environmental sensors operated independently from the rest of the collar and there are times when no environmental data are available, reducing the number of river events and migration events from the original 447 and 26 to 325 and 17 (humidity) and 331 and 21 (temperature) (Fig. 1k,l). Numbers in figure panel.

Collar environmental sensors shut down and restarted unexpectedly, possibly due to moisture penetration into the electronics. However, a median humidity and ambient temperature over time was calculated from the collar data available at that time (data from between 1 and 14 individuals, typically 6-8). Minimum and maximum values were extracted using a peak detection algorithm and median daily maximum and minimum values were calculated for each month (Fig. 1o,p). Those medians over the course of the month contain data from 5-14 individuals for humidity and 6-14 individuals for ambient temperature.

Runs

Stride parameters, such as speed and frequency, were calculated from the triggered high resolution data¹⁰. GPS-INS (Global Positioning System-Inertial Navigation System) processing was used to reduce noise and improve precision for the position and velocity analysis, as well as increase the temporal resolution of the data. GPS and IMU measurements were fused using a 12-state extended Kalman filter in loosely coupled architecture^{10,25}. For the combined GPS-IMU data, the position accuracy was estimated to be 0.30 m and speed accuracy to be 0.17 m s⁻¹.

Vertical accelerations were used to determine stride times^{10,25}. Stride frequency was calculated from the time between acceleration peaks and divided by two for symmetrical gaits. Horizontal stride speed was derived from the Kalman-filtered velocity averaged over each stride in order to remove the effects of speed fluctuation through the stride and collar oscillation relative to the centre of mass. Stride speed was weighted with the preceding and following stride to remove outliers^{10,27,28}. Gait was assigned based on speed thresholds: walking for speeds up to 1.8 m s⁻¹, trot between 1.8 m s⁻¹ and 4.7 m s⁻¹ and running above 4.7 m s⁻¹. Dimensionless speed was $\sqrt{(\text{leg length} \times 9.81)^{16}}$.

Muscle: Fibre bundles from wildebeest and cow

Measurement of energy use at a muscle level, rather than a whole animal level (oxygen consumption), is challenging. The most direct approach is to measure the mechanical work and heat released by a working fibre bundle during contraction. The individual temperature changes are small (around 0.001°C) and rapid, and thus require highly sensitive custom-made thermopiles and a stable “baseline” temperature. To characterise a muscle an extensive series of measurements on living tissue with a viable cell membrane are required. Fibre bundles are dissected by hand and are particularly difficult to secure from large mammals because most of their fibres are very long and always small in diameter (less than about 100 µm). Most published measurements on mammals have therefore been on laboratory rodents.

Fibre bundles from *flexor carpi ulnaris* with aponeurosis (tendon) at each end were dissected from biopsies in saline (composition (mmol l⁻¹): NaCl 135, KCl 4.0, CaCl₂ 2.35, MgCl₂ 0.85, NaH₂PO₄ 1.0, NaHCO₃ 20 and glucose 5.5 and equilibrated with 95% O₂ + 5% CO₂).

Aluminium foil t-shaped clips were attached to the tendons. The fibre preparation was mounted on a vertical thermopile between a fixed hook and a stainless-steel wire connected to the lever arm of a combined motor and force transducer (Series 300B Lever System and Series 400A Force Transducer System, Cambridge Technology, Inc., Watertown, MA, USA).

Experiments were performed at 25°C rather than at body temperature (38°C) for consistency with other studies and because muscle preparations tend to be more resilient at lower temperatures. Muscle shortening velocity and power are temperature-dependent with a Q₁₀ in the order of 2.3²⁹; this equates to a three-fold increase from our measurements at 25°C to the physiological temperature of 38°C. The effect on optimum cycle frequency has not been defined so we applied a more cautious twofold difference. Efficiency is temperature independent³⁰.

The fibre bundle was stimulated electrically (Isolated Stimulator Model DS2, Digitimer, Ltd., Welwyn Garden City, Herts, UK). Supra-maximal stimulus strength (at 60 Hz, 2 ms pulse⁻¹) and L_o , the fibre length giving maximum active force, were found for each fibre bundle at the start of the experiment. The motor either held the fibre bundle at constant length (isometric) or imposed cycles of sinusoidal movement at 0.5 Hz. and peak-to-peak amplitude of about 18% L_o (Extended Data Fig. 2a). Stimulation consisted of three tetani, each lasting for part of the 2.0 s movement cycle (stimulation duty cycle, DC = 0.1, etc). The stimulation phase (timing of the tetanus within the movement cycle) was varied in steps of 0.1 of the movement cycle. See Extended Data Fig. 2 for values of movement amplitude, stimulation DC and phase for wildebeest and cow. Passive force was recorded during sinusoidal movement

without stimulation and was subtracted from the force produced during stimulation to give the active force. Isometric contractions were performed at intervals during the experiments. The duration of stimulation in these isometric contractions was 0.8 s corresponding to DC 0.4 of the movement cycle duration for the fibre bundle.

Energetic Measurements: Wildebeest

Muscle biopsies were obtained as described in the main text. Muscle temperature was measured by a custom-made thermopile (D1) consisting of antimony-bismuth thermocouples (Seebeck coefficient, $90.2 \mu\text{V } ^\circ\text{K}^{-1} \text{ couple}^{-1}$). The outputs from each of three 2-mm sections of the thermopile (8 couples per section) were recorded separately. A LabView program (National Instruments Corporation, Austin, TX USA) controlled the stimulator and motor, and also recorded force, lever position, and the outputs from the three thermopile sections. The program interfaced to the instruments using a USB-6229 DAQ (National Instruments Corporation, Austin, TX, USA).

Successful energetic measurements were made on 5 muscle fibre bundles from 4 wildebeests (Fig. 3, Extended Data Fig. 4 and Extended Data Table 4). Pooling the data for the two bundles from the same wildebeest yields a mean peak efficiency of 62.6% ($n=4$, range 57.3 to 66.6). Removing the data for the bundle 3B (Extended Data Fig. 4f, Extended Data Table 4b) which had unexplained very low values for all parameters gives a higher mean peak efficiency of 64.2% ($n=4$, range 60.2-66.6) and averaging the second highest efficiency value determined for each of these four bundles give a mean of 62.6% (range 59.8-65.8) giving confidence that 62.6% is a robust measure of wildebeest muscle efficiency. Note that a fibre bundle's peak efficiency is its highest value among all DCs and phases tested, whereas Fig. 3 shows the means for each combination of DC and phase.

Energetic Measurements: Cow

We used a thermopile, D2, which was similar to D1 described above. The Seebeck coefficient for D2 was $97.5 \mu\text{V } ^\circ\text{K}^{-1} \text{ couple}^{-1}$ and D2 was longer and therefore more suitable for the longer fibre bundles from Cow. Records were made from either 1, 2 or 3 thermopile sections (8 couples per section, 2 mm per section) depending on the bundle length and on its position on the thermopile. Force was recorded as described for wildebeest.

Samples of the *flexor carpi ulnaris* were also retrieved from 7 adult cows killed at a local abattoir. We report results for muscle samples from 5 of these cows (mean estimated body mass $760 \text{ kg} \pm \text{sd } 23$, $n=5$; mean leg length to top of scapula $1.43 \text{ m} \pm \text{sd } 0.11$, $n=5$). Leg length to insertion of *serratus ventralis* (same as wildebeest) was taken as 150 mm less, ie 1.28 m. Muscle samples from 2 of the cows did not complete enough of the protocol to be included.

Fibre bundle size

After all the records had been made, a digital photograph was made of the fibre bundle at L_o on the thermopile. The clip-to-clip length was measured from the image. The fibre bundle was pinned in a dissecting dish at the L_o clip-to-clip length and fixed in ethanol. The clips and tendon were removed and the fibre length was measured under the stereomicroscope. The fibre bundle was weighed after drying in room air. Dry mass/blotted mass was assumed to be

same as we have measured for bundles of fibres from wild rabbit, $0.188 \pm \text{sem } 0.009$, $n=8$. Cross sectional area (CSA) was evaluated as blotted mass/ L_o .

Work, Heat, Efficiency and Impulse

Recording for wildebeest and cow fibre bundles were analysed in the same way. Work was calculated as the integral of active force and length change. Impulse was calculated as the integral of active stress and time. Heat loss was evaluated using the time constant for heat loss measured by the Peltier method^{31,32}. Heat production was calculated from the thermopile output plus heat lost, using the Seebeck coefficient, number of thermocouples, and the heat capacity of the fibre bundle evaluated from its mass and a specific heat capacity of $3.668 \mu\text{J } ^\circ\text{mK}^{-1} \text{mg}^{-1} \text{muscle}$ ³³. Stimulus heat was measured after the muscle fibres had been made unexcitable with procaine (30 mmol l^{-1} in saline). The heat values are reported as net of stimulus heat.

Work, heat and impulse produced in three complete cycles of movement (6 s) were measured. Work values are the “net” work, which is the sum of work done by the muscle during shortening less the work done on the muscle by the motor during stretch. Power values are the net work in 3 cycles of movement/duration of 3 cycles, in other words, the average power produced during this 6 s period. Work, power and heat are reported per kg of muscle. Efficiency was evaluated as net work/heat + net work. Comparable efficiency results from literature are shown Extended Data Table 5. Impulse is reported as stress x time ($\text{mN s per mm}^2 = \text{kPa s}$). The cost per unit impulse was compared with that of rat muscle by performing equivalent calculations on the data reported in³⁴ (see Extended Data Table 3b).

Comparable data were drawn from literature and tabulated in Extended Data Table 5.

References^{11,17,30,35,36,37}.

Fatigue and recovery

Tests of fatigue and recovery were done on some of the fibre bundles of wildebeest muscle. In our standard isometric protocol described above the fibre bundle performed 3 cycles consisting of 0.8 s stimulation followed by 1.2 s without stimulation. To examine fatigue and recovery of isometric stress we repeated 25 (or 50) cycles with stimulation, followed by a 10 (or 30) min recovery, then a test cycle with stimulation. Two sets of results from different fibre bundles are reported for the 25 stimulation cycles + 10 min recovery protocol, and one set of results for the 50 stimulation cycles + 30 min recovery protocol. After 25 contraction cycles peak force fatigued to about 50% and after 50 cycles to 37% of its initial value (Fig. 3i). After the recovery period the initial force was completely restored; recovered/initial peak force = $1.001 \pm \text{sem } 0.004$, $n=3$ (Fig. 3j).

Calculation of cross-bridge work from efficiency

The costs associated with Ca^{2+} reactions in wildebeest muscle may be low and contribute to high efficiency, but this could not be evaluated with the design of experiment we used. To get some insight into the role of the cross-bridge cycle in efficiency, we have applied the principles set out by Barclay¹⁹ (Extended Data Table 6). Each cross-bridge cycle uses one ATP making 100 zJ ($z=10^{-21}$) of free energy available for conversion to mechanical work. However, measurements of the distance over which a cross-bridge is attached and the force it

produces show that only 50 zJ of mechanical work can be done in a cross-bridge cycle. Such measurements have been made on muscle fibres from frog, dogfish and rat; the values are consistent and appear to be a fundamental property of the cross-bridges in vertebrate muscle. What varies between different muscles and muscles from different species is the fraction of theoretically possible 50 zJ that is actually converted to work (Extended Data Table 6c). In mechanistic terms, a work per cross-bridge value less than 50 zJ means that when the cross-bridge attaches and detaches, it does so at locations that do not yield maximum work. In other words, the attached cross-bridge traverses only part of its force-length relationship in each cycle. We have calculated the cross-bridge work for wildebeest and cow muscle using our measured efficiency values and have assumed that the other required parameters are within the ranges measured for other muscles (Extended Data Table 6d,e).

Calculation of net COT, water and heat balance of a 220 kg wildebeest Taylor⁵ presents COT data for a blue wildebeest of body mass 92 kg and an eland of 213 kg and also a regression line derived from COT data for 11 species of artiodactyl. We used the regression line for the artiodactyls to get a whole animal net (ie above resting metabolism) COT of 379 J m⁻¹ for our 220 kg wildebeest. For comparison, the eland equation gave a net 220 kg whole animal COT of 367 J m⁻¹ and the somewhat smaller 92 kg wildebeest value 407 J m⁻¹ which were considered close enough to rely on the regression line prediction.

Taking an oxygen equivalent of 20.1 J per ml O₂ (20.1 kJ L⁻¹)² gives an oxygen consumption of

$$0.379 \times 10^3 / 20.1 = 18.9 \text{ litres O}_2 \text{ per km.}$$

Assuming a 5% oxygen extraction from air (data for horses walking on a treadmill²⁰) this would require an additional ventilation of

$$18.9/0.05 = 378 \text{ L} = 0.378 \text{ m}^3 \text{ per km}$$

In this study system locomotion occurred during hot, dry times of the day so there is water loss due to saturating the extra ventilation with water in the lungs. Saturating that volume of air with water vapour at 38°C (body temperature) and initial humidity of 12% (October median minimum humidity at about the same temperature, Fig 1o).

The maximum water content of air increases with temperature and can be sourced from engineering tables (eg Handbook of Chemistry and Physics). At 38°C it is 45.7 g H₂O m⁻³ of air and taking 0.378 m³ of air from 12% to 100% humidity requires

$$0.88 \times 45.7 \times 0.378 = 15.2 \text{ ml of water (per km).}$$

Respiratory water loss is offset somewhat by metabolic production due to oxidation of carbohydrates (0.0317 g H₂O per kJ) and fats (0.0290 g H₂O per kJ). Using the mean of these (0.0304 g per kJ) yields 11.5 mL/km water from 379 kJ/km energy expenditure.

$$0.0304 \times 379 \times 1000 = 11.5 \text{ ml H}_2\text{O per km walked.}$$

Adding this to the respiratory water loss of 15.2 ml km^{-1} gives a net extra water loss due to locomotion of:

$-15.2 + 11.5 = -3.7 \text{ ml km}^{-1}$. So 74 ml day^{-1} (0.074 l day^{-1}) when walking 20 km per day.

Ambient temperature often exceeded 38°C between September and December (Fig. 1p, Extended Data Fig. 1) and the substantial radiant heat load in these environments will add to the requirement for evaporative cooling. When walking on the level, most energy (heat + work) generated within muscles turns to heat within the animal - except for work done disturbing the environment. Dehydrated animals may store some heat during the day with a rise in temperature^{21,38}, allowing it to dissipate at night. Only small fluctuations of about 1°C are observed in wildebeest. A 220 kg animal with a thermal capacity around 80% that of water¹ ($3.34 \text{ kJ/kg/}^\circ\text{C}$) could store just 0.73 MJ of heat with a 1°C rise, less than 10% of the 7.58 MJ generated by walking 20km. So daytime dissipation is essential, requiring evaporation of much more water than evaporates with minimal ventilation.

Walking 20 km generates 7.58 MJ of heat.

This heat which would be dissipated by evaporating water (heat of vapourisation 2257 J g^{-1}). $7.58 \times 10^6 / 2257 = 3360 \text{ ml} = 3.36 \text{ litres}$ of water. Some of this can be the respiratory water loss.

Subtract metabolic water gain of 0.23 litres ($0.0115 \text{ l km}^{-1} \times 20 \text{ km}$)

So in hot conditions net extra water loss due to locomotion (after metabolic water gain of 230 ml) would rise from 0.074 l to 3.13 l per 20 km walked.

Additional water loss due to basal metabolism - not directly associated with walking - is uncertain. A wildebeest grazing in Kenyan arid equatorial grassland in winter had a daily water turnover/requirement of $54 \text{ ml kg}^{-1}\text{day}^{-1}$ ²³ (5.4% body mass/day), measured on an animal (1° South of equator)³⁹ ie for a 220 kg animal:

$220 \times 0.054 = 11.9 \text{ litres day}^{-1}$

These data are supported by measurements of wildebeest water requirements in a temperature controlled room fluctuating between 22 and 40°C ($10.6 \text{ litres per day}$, $n=3$)³⁹. During migration and dehydration, animals may however use less water for digestion and excretion.

Walking 20 km a day in cool conditions would increase net water loss (by the respiratory route due to increased ventilation for gas exchange – ($0.074 \text{ l H}_2\text{O}$) by $0.074/11.9 = 0.6\%$ so an increase of only 0.6% in water utilisation.

In hot conditions if 3.13 litres of water is evaporated for thermoregulation (the complete heat load) this would rise to $11.9 + 3.13 = 15 \text{ litres}$ an increase of $3.13/11.9 = 26\%$ in daily water utilisation.

Animals become debilitated through dehydration when they reach around 20% body mass loss though some animals can survive 30% weight loss²⁴. Assuming this weight loss is all water – some will actually be body fat and ingesta. Ruminant contents can contain much water which may buffer body water to some extent aiding survival.

$0.2 \times 220 \text{ kg} = 44 \text{ litres}$ of water loss will result in 20% dehydration

At a water loss rate of 11.9 litres per day this would happen in just under four days (44/11.9). For a wildebeest walking 20 km per day in hot conditions 20% dehydration would occur in three days (44/15).

If wildebeest muscle efficiency was the same as the value we measured for substantially larger cows (41.8%, Table 1) rather than 62.6%, then to generate the same mechanical work (which is converted to heat in the body) the COT and oxygen requirement would increase by $62.6/41.8 = 1.50$ times

This would result in a concomitant increase in ventilation and net water loss by that route $0.074 \times 1.5 = 0.11 \text{ l day}^{-1}$ in cool conditions.

The total heat generated would increase by the same amount

$1.5 \times 7.58 \text{ MJ} = 11.4 \text{ MJ}$

This would require a net thermoregulation evaporation of

$11.4 \times 10^6 / 2257 = 5.1 \text{ l day}^{-1}$ in hot conditions.

This would equate to a higher daily water requirement of

$11.9 + 5.1 = 17.0 \text{ l day}^{-1}$

This is a 13% rise (17.0/15.0) in daily water requirement.

Data availability

The authors declare that all relevant processed data supporting the findings of this study are available as Source Data files. Further data are available from the corresponding authors upon reasonable request.

References

- 25 Wilson, A.M., Hubel, T.Y., Wilshin, S.D., Lowe, J.C., Lorenc, M., Dewhirst, O.P. et al. Biomechanics of predator–prey arms race in lion, zebra, cheetah and impala. *Nature* **554**, 183-188 (2018).
- 26 Dewhirst, O.P., Evans, H.K., Roskilly, K., Harvey, R.J., Hubel, T.Y. and Wilson, A.M. Improving the accuracy of estimates of animal path and travel distance using GPS drift- corrected dead reckoning. *Ecol Evol.* **6**, 6210-6222 (2016).
- 27 Hubel, T.Y., Myatt, J.P., Jordan, N.R., Dewhirst, O.P., McNutt, J.W., Wilson, A.M. Energy cost and return for hunting in African wild dogs and cheetahs. *Nat Commun.* 2016;11034.
- 28 Hubel, T.Y., Myatt, J.P., Jordan, N.R., Dewhirst, O.P., McNutt, J.W., Wilson, A.M. Additive opportunistic capture explains group hunting benefits in African wild dogs. *Nat Commun.* 2016;11033.
- 29 West, T.G., Toepfer, C.N., Woledge, R.C., Curtin, N.A., Rowleson, A., Kalakoutis, M. et al. Power output of skinned skeletal muscle fibres from the cheetah (*Acinonyx jubatus*). *J Exp Biol.* **216**, 2974-2982 (2013).

- 30 Barclay, C.J., Woledge, R.C., Curtin, N.A. Is the efficiency of mammalian (mouse) skeletal muscle temperature dependent? *J Physiol.* **588**, 3819-3831 (2010).
- 31 Kretzschmar, K., Wilkie, D. The use of the Peltier effect for simple and accurate calibration of thermoelectric devices. *Proc R Soc Lond B.* **190**, 315-321 (1975).
- 32 Woledge, R.C., Curtin, N.A., Homsher, E. Energetic aspects of muscle contraction. *Monogr Physiol Soc.* **41**,1-357 (1985).
- 33 Hill, A. *Trails and Trials in Physiology*. London: E. Arnold Ltd.; 1965.
- 34 Phillips, S., Takei, M., Yamada, K. The time course of phosphate metabolites and intracellular pH using ³¹P NMR compared to recovery heat in rat soleus muscle. *J Physiol.* **460**, 693-704 (1993).
- 35 Curtin, N.A. & Woledge, R.C. (1993). Efficiency of energy conversion during sinusoidal movement of white muscle fibres from the dogfish, *Scyliorhinus canicula*. *J. exp. Biol.* **183**, 137-147.
- 36 Barclay, C.J. (1996). Mechanical efficiency and fatigue of fast and slow muscles of the mouse. *J. Physiol.* **497**, 781-794.
- 37 Curtin, N.A. & Woledge, R.C. (1991). Efficiency of energy conversion during shortening of muscle fibres from the dogfish, *Scyliorhinus canicula*. *J. exp. Biol.* **158**, 343-353.
- 38 Hetem, R.S., Strauss, W.M., Fick, L.G., Maloney, S.K., Meyer, L.C.R., Shobrak, M. et al. Variation in the daily rhythm of body temperature of free-living Arabian oryx (*Oryx leucoryx*): does water limitation drive heterothermy? *J Comp Physiol B.* **180**, 1111-1119 (2010).
- 39 Maloiy, G.M.O. Water metabolism of East African ruminants in arid and semi- arid regions. *Zeitschrift für Tierzüchtung und Züchtungsbiologie* **90**, 219-228 (1973).

Animal name	Start date	End date	Number of days
G690	16-May-2016	27-Oct-2017	529
G692	17-May-2016	10-Apr-2017	328
G693	18-May-2016	17-Nov-2017	548
G694	18-May-2016	16-Nov-2017	547
G695	18-May-2016	14-Nov-2017	545
G696	18-May-2016	14-Nov-2017	545
G697	19-May-2016	18-Nov-2017	548
G698	19-May-2016	22-Aug-2016	95
G699	19-May-2016	19-Nov-2016	184
G700	19-May-2016	31-Aug-2017	469
G701	19-May-2016	13-Nov-2017	543
G702	30-Jul-2016	07-Nov-2017	465
G703	30-Jul-2016	09-Nov-2017	467
G704	20-May-2016	31-Jan-2017	256
G705	30-Jul-2016	09-Nov-2017	467
G706	31-Jul-2016	09-Nov-2017	466
G709	31-Jul-2016	08-Feb-2017	192

Extended data Table 1. Subject data. Start and end date for data collection and number of days data collected for each individuals. Individual G690 did not migrate but remained in wet season range throughout the study so only provided data for gait analysis.

a	DC	0.4	0.3	0.2	0.1	c	DC	0.3	0.2
	Phase						Phase		
	-0.2	4	4	4	4		-0.2	3	2
	-0.1	4	4	4	4		-0.1	5	5
	0	4	4	4	4		0	5	5
	0.1	3	4	4	4		0.1	5	5
	0.2	2	2	2	3				
	0.3				2				

b	DC	0.4	0.3	0.2	0.1	d	DC	0.3	0.2
	Phase						Phase		
	-0.2	4	4	4			-0.2	3	2
	-0.1	4	4	4	4		-0.1	5	5
	0	4	4	4	4		0	5	5
	0.1	2	4	4	4		0.1	4	5
	0.2		2	2	3				

Extended Data Table 2. N values. **a** for wildebeest and **c** for cow, n values for mean power, impulse and cost per unit impulse in Figure 3 a,c,d,e,g, and h. **b** for wildebeest and **d** for cow, n values for mean efficiency in Figure 3 b and f. Note that efficiency was not calculated when net work was negative.

	Sinusoidal movement	Wildebeest	Cow
		Isometric	Isometric
a			
Mean	0.056	0.068	0.080
Stdev.s	0.022	0.043	0.027
SEM	0.011	0.021	0.012
n	4	4	5

b	Animal	Dur (s)	Initial heat (J/kg)	Impulse (kPa s)	Cost/impulse (J/kg/kPa/s)
	Rat	2	27.1	372	0.073
	Rat	4	51.6	744	0.069
	Wildebeest	2.4	20.4	274.6	0.068
	Cow	2.4	25.0	314.4	0.080

Extended Data Table 3a. Minimum cost per unit impulse ($\text{J kg}^{-1}/(\text{s} \times \text{kPa})$). Mean minimum values (1 value fibre bundle) for contractions with sinusoidal movement at any of the tested DCs and phases (wildebeest) and during isometric contraction at stimulation DC 0.4 (wildebeest and cow).

Extended Data Table 3b. Comparison of cost per unit impulse of rat, wildebeest and cow muscle fibre bundles. Rat values are based on earlier report (Phillips et al, 1993³⁴). Dur is the duration of stimulation under isometric conditions. For rat isometric stress was 186 kPa (based on wet mass), having been converted from the reported value of 0.93 N m g^{-1} dry mass, using wet mass/dry mass = 5. Impulse was dur x isometric stress. Wildebeest and cow values are reported here. See text and isometric values (down triangles) in Fig. 3 d&h. Dur = 3 contractions x 0.8 s per contraction.

a	animal-bundle code	max ϵ	net work (J/kg)	enthalpy (J/kg)	avg power (W/kg)	avg enthalpy rate (W/kg)	DC	phase
	Wildebeest							
	1A	0.662	11.76	17.76	1.96	2.96	0.2	-0.1
	2A	0.666	11.57	17.36	1.93	2.89	0.3	0
	3A&B	0.573	13.03	21.58	2.17	3.60	0.2	0
	4A	0.602	30.40	50.52	5.07	8.42	0.1	0.1
	mean	0.626	16.69	26.80	2.78	4.47		
	stdev.s	0.046	9.16	15.93	1.53	2.65		
	sem	0.023	4.58	7.96	0.76	1.33		
	n	4	4	4	4	4		
b	animal-bundle code	max ϵ	net work (J/kg)	enthalpy (J/kg)	avg power (W/kg)	avg enthalpy rate (W/kg)	DC	phase
	Wildebeest							
	3A	0.636	20.48	32.20	3.41	5.37	0.2	0
	3B	0.510	5.59	10.96	0.93	1.83	0.2	0
c	animal-bundle code	max ϵ	net work (J/kg)	enthalpy (J/kg)	avg power (W/kg)	avg enthalpy rate (W/kg)	DC	phase
	Cow							
	1	0.415	20.75	50.05	3.46	8.34	0.2	0
	2	0.373	6.47	17.35	1.08	2.89	0.2	0
	3	0.443	4.79	10.80	0.80	1.80	0.2	-0.1
	4	0.432	8.52	19.73	1.42	3.29	0.2	-0.1
	5	0.429	11.93	27.82	1.99	4.64	0.2	-0.1
	mean	0.418	10.49	25.15	1.75	4.19		
	stdev.s	0.027	6.32	15.19	1.05	2.53		
	sem	0.012	2.83	6.79	0.47	1.13		
	n	5	5	5	5	5		

Extended Data Table 4. Maximum enthalpy efficiency (max ϵ) value for muscle fibre bundles from wildebeest and cow. a and b, wildebeest. c, cow. Animal-bundle code: digit indicates the animal, letter indicates the fibre bundle from that animal. In A, line 3A&B lists averages of the results for two fibre bundles, A and B, from the same wildebeest, 3. In B, the results of these fibre bundles, 3A and 3B, are listed separately. The table lists the max ϵ , the duty cycle and phase at which it was produced and the net work, enthalpy, power and enthalpy rate produced in the max ϵ condition (maximum ϵ value from all DCs and phases tested on the muscle fibre bundle, see Extended Data Fig. 2). Enthalpy efficiency (ϵ) is the net work/enthalpy produced by the muscle during 3 cycles of sinusoidal movement at 0.5 Hz with stimulation during part of each movement cycle. Net work is the sum of the work done during the shortening part and the lengthening part of the movement cycles. In this context work done during shortening is taken to be positive, and that during lengthening to be negative. Enthalpy is the sum of net work and heat production. Work is the integral of active force and length change. Active force is the total force produced with stimulation – that produced without stimulation. Av power is average power in 3 cycles of movement = work / 6 s. Av enthalpy rate = enthalpy produced in 3 cycles of movement/6 s. DC (stimulation duration in s in one cycle/2 s cycle time) and stimulation phase (= (stimulation start time-shortening start time)/2 s cycle time).

animal	max ϵ	(sem; n)	design	move freq (Hz)	muscle	ref
wildebeest	0.626	(\pm 0.023; 4)	C	0.5	flexor carpi ulnaris	this ms
cow	0.418	(\pm 0.012; 5)	C	0.5	flexor carpi ulnaris	this ms
dogfish	0.41	(\pm 0.02; 13)	C	2 & 2.5	white myotomal	Curtin & Woledge (1993)
mouse	0.34	(\pm 0.03; 4)	C	8	extensor digitorum longus	Barclay (1994)
mouse	0.52	(\pm 0.01; 4)	C	3	soleus*	Barclay (1994)
wild rabbit	0.266	(\pm 0.041; 5)	C	1 or 2	extensor digiti V & peroneus longus	in preparation
tortoise	0.77	(\pm 0.02; 8)	I		rectus femoris	Woledge (1968)
mouse	0.26	(\pm 0.01; 5)	I		extensor digitorum longus	Barclay et al (2010)
mouse	0.333	(\pm 0.02; 6)	I		extensor digitorum longus	Barclay (1996)
mouse	0.425	(\pm 0.025; 6)	I		soleus*	Barclay (1996)
dogfish	0.312	(\pm 0.020; 6)	I		white myotomal	Curtin & Woledge (1991)

Extended Data Table 5. Values of maximum enthalpy efficiency (ϵ) for locomotor muscles from different species. * indicates antigravity muscle. Measurements were all made on intact fibres bundles. Design C: cyclic movement at the listed frequency and with intermittent stimulation. Design I: isotonic (=force-clamp) or isovelocity (=velocity-clamp) following a period under isometric (=constant length) conditions. In design I stimulation was continuous, and efficiency was measured only during shortening. References^{11,17,30,35-37}.

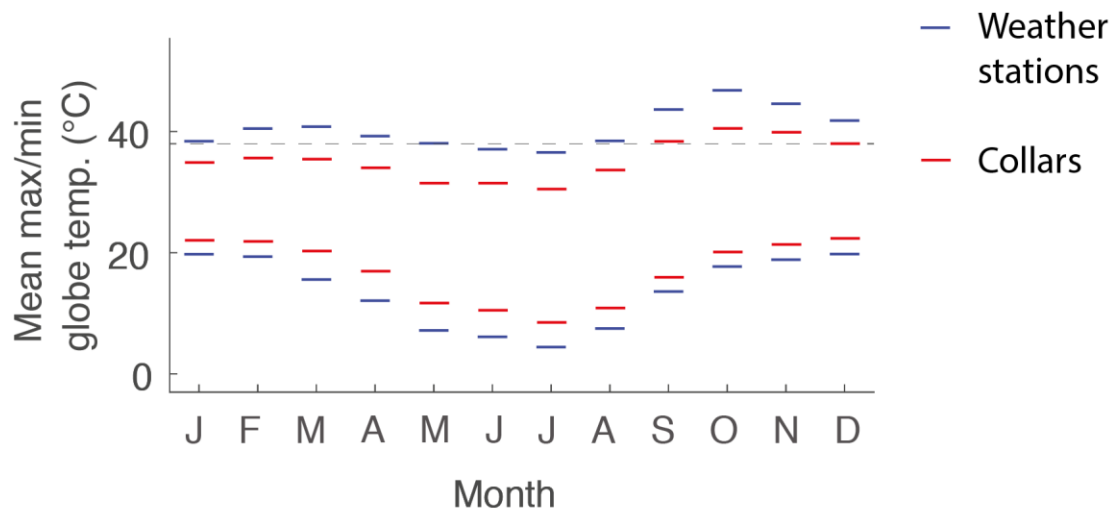
a	term	definition
	ϵ_{Max}	maximum observed initial enthalpy efficiency (work/(work+heat) or power/(power+heat rate))
	enthalpy	work + heat
	η_{CB}	cross-bridge thermodynamic efficiency
	g	rate of enthalpy output at max ϵ , expressed relative to the rate of enthalpy output in isometric contraction
	f_A	activation heat rate/isometric heat rate
	$g-f_A$	the non-activation rate of enthalpy output at max ϵ , expressed relative to the rate of enthalpy output in isometric contraction.
	ΔH_{Pcr}	-34 kJ/mol, molar enthalpy change of phosphocreatine hydrolysis
	ΔG_{ATP}	free energy of ATP hydrolysis for conditions in muscle, -60.5 kJ/mol, 100 zJ per molecule of ATP
	W_{CB}	maximum measured work output per cross-bridge ATP-splitting cycle, units = zJ
	W_{max}	50 zJ, the theoretical maximum cross-bridge work per attachment cycle: area under the cross-bridge force-extension curve; derived from the T2 curve. See Fig. 16 Barclay (2015)
	W_{CB}/W_{max}	fraction of the theoretically maximum cross-bridge work that is actually achieved by the muscle

b	equation	definition	c	Species	ϵ_{Max}	$Max \eta_{CB}$	W_{CB} (zJ)	W_{CB}/W_{max} (%)
	$Max \eta_{CB}$	$= \epsilon \times (g/g-f_A) \times (\Delta H_{Pcr}/\Delta G_{ATP})$		Dogfish white	0.33	0.22	21.6	43
	W_{CB}	$= \eta_{CB} \times \Delta G_{ATP}$		Mouse Edl	0.26	0.19	18.5	37
				Tortoise	0.77	0.46	45.8	92

d	Species	ϵ_{Max}	g	f_A	ΔH_{Pcr}	ΔG_{ATP}	η_{CB}	W_{CB} (zJ)	W_{max} (zJ)	W_{CB}/W_{max} (%)
	Wildebbeest	0.626	1.9	0.345	34.0	60.5	0.430	42.99	50	86%
		0.626	2.5	0.345	34.0	60.5	0.408	40.81	50	82%
		0.626	5.30	0.345	34.0	60.5	0.376	37.63	50	75%
		0.626	5.3	0.27	34.0	60.5	0.410	41.01	50	82%
		0.626	2.5	0.27	34.0	60.5	0.394	39.44	50	79%
		0.626	5.30	0.27	34.0	60.5	0.371	37.07	50	74%

e	Species	ϵ_{Max}	g	f_A	ΔH_{Pcr}	ΔG_{ATP}	η_{CB}	W_{CB} (zJ)	W_{max} (zJ)	W_{CB}/W_{max} (%)
	Cow	0.418	1.9	0.345	34.0	60.5	0.287	28.70	50	57%
		0.418	2.5	0.345	34.0	60.5	0.273	27.25	50	55%
		0.418	5.30	0.345	34.0	60.5	0.251	25.13	50	50%
		0.418	1.9	0.27	34.0	60.5	0.274	27.38	50	55%
		0.418	2.5	0.27	34.0	60.5	0.263	26.34	50	53%
		0.418	5.30	0.27	34.0	60.5	0.248	24.75	50	50%

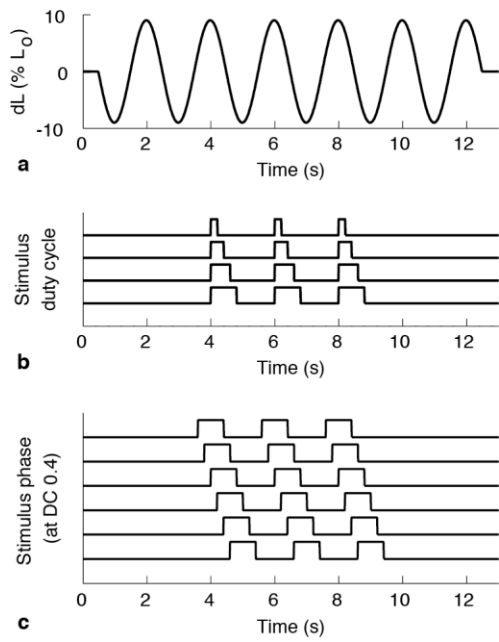
Extended Data Table 6. Calculation of cross-bridge work from enthalpy efficiency. Based on Barclay (2015)¹⁹. (a) Definitions of terms. (b) Equations. (c) Values for muscle from 3 species. $Max \eta_{CB}$ and W_{CB} were calculated from the equations in (b) using values of g and f_A given¹⁹ Table 11. W_{max} is 50 zJ, the theoretical maximum cross-bridge work per attachment cycle. (d) Maximum enthalpy efficiency and work values for wildebeest muscle. ϵ_{Max} 0.626 is the maximum enthalpy efficiency. η_{CB} and W_{CB} were calculated using the equations in (b). We have assumed that our ϵ_{Max} from cyclic movement experiments also applies in isotonic or isovelocity experiments (see supporting evidence in Extended Data Table 5). The values of g and f_A are all combinations of the values for dogfish white fibres, mouse EDL fibres, and tortoise rectus femoris muscle (see Table 11 of¹⁹). W_{CB}/W_{max} is the work actually done by the cross-bridge as a % of the theoretically maximum cross-bridge work. The highest and lowest values of W_{CB}/W_{max} are in bold font. (e) Values for cow fibre bundles corresponding to those described in (d).



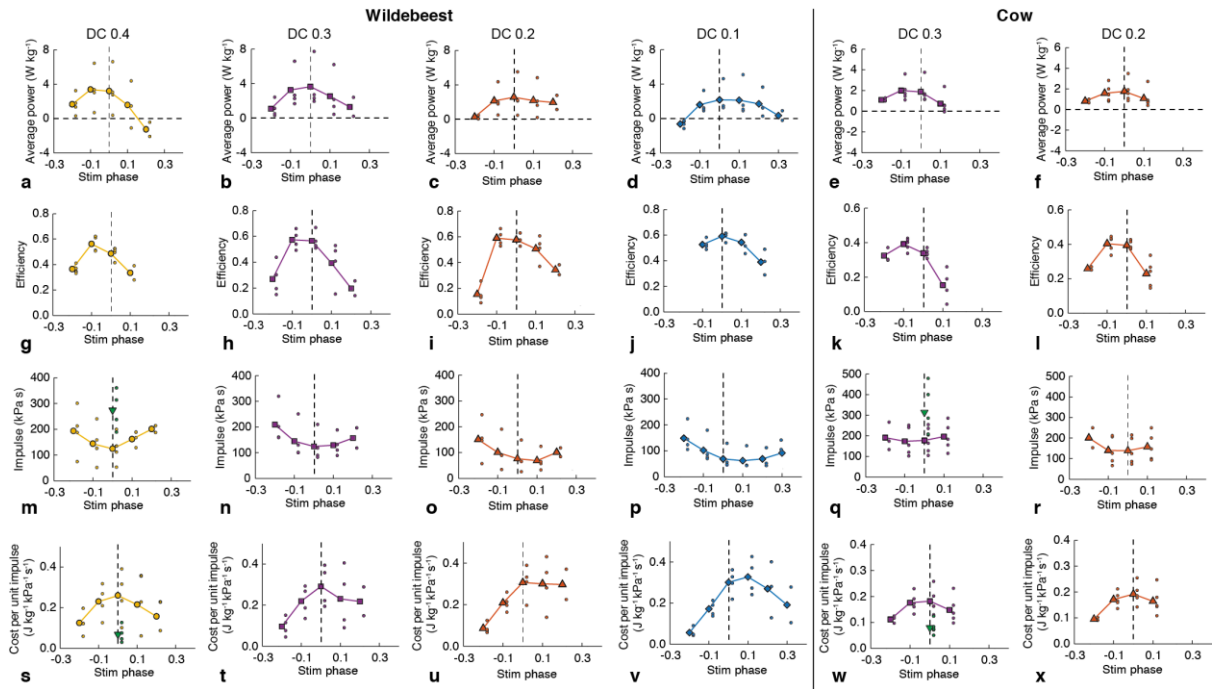
Extended Data Figure 1. Comparison of temperature maxima and minima recorded on collars and on weather stations.

Number of collar sensors working varied so a median was taken from all available data on each day and the maximum and minimum value for each day then averaged over each month.

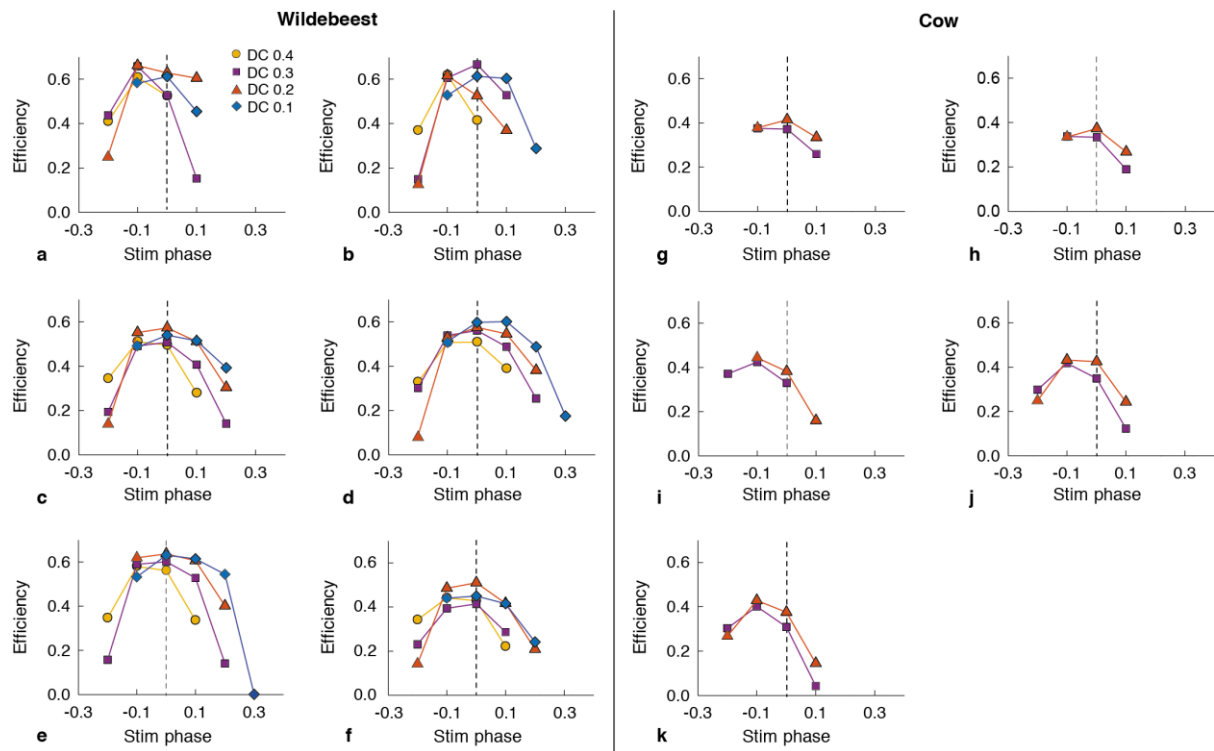
Monthly maximum Temperature was $5.6 \pm \text{SD } 0.6^\circ\text{C}$ higher on the weather stations than the collars and monthly minimum temperature was, on average, $3.6 \pm 1.1^\circ\text{C}$ lower on the weather stations than the collars. Both mean \pm SD, $n=12$). Ambient temperature exceeded body temperature of 38°C (horizontal dashed line) on nine months of the year. Note weather stations were 10 km away from the river in the dry season range whilst animals were in the wet season range to the East from November to April approximately. (Figure 1b,c).



Extended Data Figure 2. Controlled variables: muscle length and stimulation pattern. **a**, pattern of lever movement. Values for cow experiments are in parentheses where they are different than those for wildebeest. Frequency 0.5 Hz and peak-to-peak amplitude 18% L_o (10% L_o). L_o is the fibre bundle length at which isometric force was greatest. **b**, stimulus duty cycles (DC) used in the experiments. Top to bottom: DC 0.1, 0.2, 0.3, and 0.4 (0.2 and 0.3). **c**, stimulus phases used in the experiments. Top to bottom: phase -0.2, -0.1, 0.0, 0.1, 0.2, and 0.3. (-0.2 to 0.1). Phase = 0.0 corresponds to the stimulus starting when shortening starts. In this example, DC = 0.4.



Extended Data Figure 3. Individual data points for Figure 3. Data presented in Fig. 3 but subdivided by DC. Mean plotted, symbol and line colour as in Fig. 3, n given in Extended Data Table 2.



Extended Data Figure 4. Efficiency vs stimulus phase for individual muscle fibre bundles from wildebeest and cow. a-f wildebeest and g-k cow. Relationship between stimulus phase and efficiency during three cycles of movement at 0.5 Hz for stimulus duty cycles: 0.4 circle, 0.3 square, 0.2 up triangle, and 0.1 diamond. Efficiency = power per rate of heat+work output. Wildebeest panels a, b, and d, are each for a different muscle fibre bundle from a different animal. Panel c is the average of the values shown in panels e and f which are results for two fibre bundles from the same wildebeest. Each cow panel is for a different fibre bundle from a different animal.